ELSEVIER

Thermochimica Acta 340–341 (1999) 221–229

thermochimica acta

www.elsevier.com/locate/tca

A study of polyimide thermoplastics used as tougheners in epoxy resins — structure, property and solubility relationships

Shanjin Li[a], Bin-Lin Hsu[b], Fuming Li[b], Christopher Y. Li[b], Frank W. Harris[b,*], Stephen Z.D. Cheng[b]

[a]*Department of Macromolecular Science, Fudan University, Shanghai, China*
[b]*Maurice Morton Institute and Department of Polymer Science, The University of Akron, Akron, OH 44325-3909, USA*

Accepted 6 August 1999

Dedicated to the occasion of Professor David Dollimore's 70th birthday.

Abstract

A series of organo-soluble aromatic polyimides have been synthesized from four different dianhydrides and two different diamines. The main purpose of this research was to develop new toughening agents from thermoplastic polyimides for epoxy resins. Thus, the solubility of these polyimides in epoxy resins is crucial to obtain a homogeneous mixture before curing. The structure dependence of these polyimides on solubility, thermal and mechanical properties was investigated in this study. The subglass relaxation processes in polyimides were also discussed based on the non-cooperative and cooperative motion proposed by Starkweather. A suitable polyimide has been found for toughening epoxy resins.

Keywords: Polyimides; Epoxy resin; Thermoplastics

1. Introduction

There has been an increasing interest in the last decade in the use of thermoplastics as toughening agents for thermoset resins. Unlike rubber, thermoplastics used to toughen thermosets do not substantially reduce mechanical properties of the toughened thermosets such as modulus and tensile strength etc. Studies have focused on polysulfone [1–3], polyethersulfone [4,5], polyimides [6] and poly(aryl ether ketone) [7,8] with different molecular weights. In some cases, the tougheners may be end-capped with functional groups, which are capable of reacting with epoxy monomers before and during cure. Two distinct possibilities in the mixing process exist. The first possibility is that the thermoplastic completely dissolves in the epoxy resin prior to curing. During curing, phase separation is induced by the increasing molecular weight of epoxy. In this case, different phase morphologies can be obtained depending on the competition between the kinetics of phase separation and cross-linking chemical reactions, which are governed by the curing conditions, compositions, molecular weights and molecular weight distributions of tougheners. The second one is physical blending of thermoplastic particles into epoxy resins, when both components are only partially miscible or totally inmiscible. Thus, phase separation is inevitable [9].

*Corresponding author.

0040-6031/99/$ – see front matter
PII: S0040-6031(99)00266-X

Although effort has been focused in this area by several researchers, a systematic study of the correlation between the chemical structures and physical properties of tougheners and the phase morphology, failure mechanisms and fracture toughness of the cured blends has not been clearly performed.

Aromatic polyimides have been used for a variety of applications due to their outstanding mechanical, electrical and thermal properties. Owing to the superior properties such as high glass transition temperature and excellent chemical resistance, an attempt has recently been made in our laboratory to develop organo-soluble aromatic polyimides for toughening epoxy resins. However, difficulties still remain in the use of polyimides as toughners, since they are not miscible with epoxy resin. In this study, solubility, mechanical, dynamic mechanical, and fracture properties of two new series of neat tougheners have been carefully examined with regard to their correlation with chemical structure. Copolyimides have also been prepared to improve solubility and macroscopic properties.

2. Experimental section

2.1. Material synthesis

Dianhydride and diamine monomers used in this work were obtained from different commercial sources, and their chemical structures are shown as in Schemes 1 and 2. 4,4′-Oxydiphthalic anhydride (ODPA) was provided by Shanghai Synthetic Resin Research; 3,3′,4,4′-benzophenonetetracarboxylic dianhydride (BTDA) and 3,3′4,4′-biphenyltetracarboxylic dianhydride (BPDA) were purchased from Chriskev and 3,4-dicarboxyphenylhexafluoropropane dianhydride (6FDA) was purchased from Hoechst. These dianhydrides as received were dried by heating to 180°C under reduced pressure for 12 h. 1,3-*Bis*(3-aminophenoxy) benzene (APB) was purchased from Mitsui Toatsu and the 2,2′-*bis*[4-(4-aminophenoxy)-phenyl]propane (BAPP) was purchased from Chriskev. The diamines were dried at 110°C under reduced pressure for 12 h before use. The *m*-cresol solvent was obtained from Aldrich and was dried with P_2O_5 for

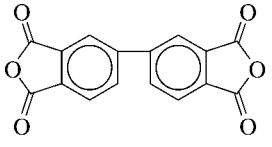

(3.3′,4,4′-bisphenyl tetracarboxylic dianhydride, BPDA)

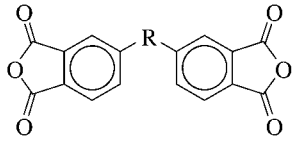

R = C = O

(3.3′,4,4′-benzeophenone tetracarboxylic dianhydride, BTDA)

R = O

(4,4′-oxydiphthalic anhydride, ODDA)

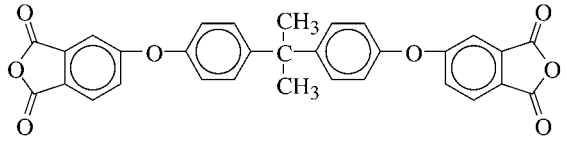

(2,2′-bis(4-(3,4-dicarboxyphenoxy) phenyl) propane, BisADA)

Scheme 1

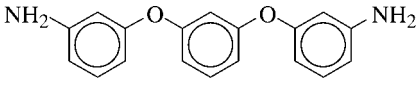

(1,3-bis (3-aminophenoxy) Benzene, APB)

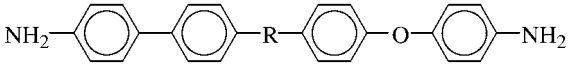

(2,2′-bis(4-(4-aminophenoxy) phenyl) propane, BAPP)

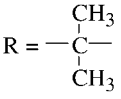

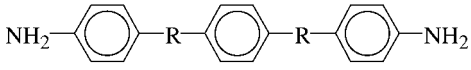

(4,4′-(1,4-phenylene-bis-(1-methyl-ethylidene)) bisaniline, Bisp)

Scheme 2

three days and distilled under reduced pressure. The Epon 828 was used as the epoxy system in this study.

The equivalent molar amount of the dianhydride was added to a diamine solution with an appropriate amount of *m*-cresol (15% w/w) which contained isoquinoline as a catalyst. The reaction was maintained at 160°C and purged with N_2 while stirring until dianhydride totally dissolved. It was then heated directly to the refluxing temperature (ca. 200°C), where it was held isothermally for 4 h. Water generated during imidization was collected by distilling off 1–3 ml of *m*-cresol. Therefore, the *m*-cresol was required to be continuously refilled to maintain the solution at a constant volume. The solution was then allowed to cool to room temperature after 4 h. The solution was slowly poured into 95% ethanol under vigorous stirring. The precipitated polymer was collected by filtration and washed several times with sufficient amount of ethanol and dried at 180–240°C (depending on the T_g of polyimide) under reduced pressured for 24 h. The inherent viscosities of the samples were measured by using a Cannon-Ubbelohde no. 100 viscometer with a *N*-methylpyrrolidinone (NMP) solution with a concentration of 0.5 g/dl at 30°C.

2.2. Instrumentation and experiments

A Seiko DSC 200 system was used to determine the glass transition temperatures (T_g) of the polyimides. Temperature and heat flow were calibrated by using indium as a standard material with a heating rate of 10°C/min. T_g measurements were taken at the point of 50% devitrification in the thermogram in which heat flow was plotted versus temperature.

Dynamic mechanical analysis (DM) experiments were carried out at heating rate of 2°C/min with a Seiko DMS 200 equipped with a cooling tank to characterize molecular relaxation of polyimides. A tensile mode was employed in these measurements and the frequencies were varied in a range from 0.1 to 10 Hz. The samples were cut to a size of $25 \times 5 \times 0.3$ mm^3 (length × width × thickness) from a molded plaque by using a diamond saw prior to testing.

The flexural modulus of each sample was measured according to the ASTM D790M-86. The double torsion (DT) fracture test was utilized to measure fracture toughness (K_{IC}) of the samples. The specimens had dimensions of $80 \times 50 \times 30$ mm^3 (length × width × thickness). A v-groove was machined onto one side of each specimen. The v-groove provides an initiation site for crack propagation through the center of the sample during fracture testing. Therefore, the loading on the specimen would lead to a primary mode I fracture upon small tip displacements.

3. Results and discussion

3.1. Solubility of the polyimides in solvents and epoxy monomers

After polymerization, the BTDA-BAPP in *m*-cresol solution shows a gel-like structure when the temperature decreases to room temperature. This gel-like structure seems to be thermally reversible because the solution returns back to the homogeneous liquid state during heating. It is speculated that when the solution cools, the solvation power is drastically decreased, and liquid-liquid phase separation may occur to form two phases of which one is solute (polymer) rich and another is solvent rich. As a result, in a concentration region of higher than about 0.5% (w/w) the solute-rich phase may form a three dimensional network, and this leads to a gel-like structure. An increase in the solvation power is achieved when the system is heated, and the gel-like structure may

thus be dissolved. Similar observations have also been made in other aromatic polyimide solution systems such as 3,6-diphenylpyromellitic dianhydride and 2,2′-*bis*(trifluoromethyl)–4,4′-diaminobiphenyl (DPPMDA-PFMB) and BPDA-PFMB in *m*-cresol [10,11]. It should be noted that the use of these aromatic polyimides having high molecular weights may lead to an increasing possibility of the phase separation owing to the fact that the entropy of mixing is substantially unfavorable in accordance with the Flory–Huggins theory [12,13]. As a result, low molecular weight polyimides (oligomers) are relatively easy to dissolve in solvents under the same chemical conditions.

Solubilities of these polyimides in various solvents and epoxy monomers were carefully examined and are listed in Table 1. As expected, both 6FDA–APB and 6FDA–BAPP are the most soluble polyimides in the solvents tested due to their strong polar interactions arising from the CF_3 groups in dianhydride portions. The increase in solubility may also be associated with the breaking of the conjugation due to the steric hindrance by twisting the two phenylenes adjacent to the CF_3 groups [14]. The ODPA-based polyimides exhibited the next highest solubility, while the BTDA- and BPDA-based polyimides were the least soluble for the series of solvents studied. One should note that differences in the molecular weights of the polymers should also be considered with regard to solubility. This is particularly important when the molecular weight is in the oligomer range. However, all the polyimides synthesized in this study are high molecular weights as documented by viscosity, GPC and light scattering measurements [15,16] (see also Table 2). Therefore, we expect that the effect of molecular weight is minimized, and difference in solubility primarily arises from the use of different dianhydrides.

Table 1
The solubility of polyimides

Polyimides	$CHCl_3$	THF	NMP	Epon-828
BPPA–APB	is[a]	is	s	is
BTDA–APB	is	is	s	is
ODDA–APB	ps[b]	is	s	s
6FDA–APB	s[c]	ps	s	s
BPPA–BAPP	is	is	s	is
BTDA–BAPP	is	is	ps	is
ODDA–BAPP	is	is	s	is
6FDA–BAPP	ps	s	s	s

[a] Insoluble.
[b] Partially soluble.
[c] Totally soluble.

Table 2
Glass transition temperature measurement of polyimides

Polyimides	η_{inh} (dl/g)[a]	T_g (°C)[b]
ODPA–APB	0.89	181
BTDA–APB	0.75	191
BPDA–APB	1.07	202
6FDA–APB	0.98	204
ODPA–BAPP	2.20	232
BTDA–BAPP	ps	240
BPDA–BAPP	2.04	250
6FDA–BAPP	1.83	258

[a] η_{inh} – inherent viscosity for polyimides were measured at 0.5 wt% in NMP at 30°C; ps – partially soluble
[b] T_g were measured from DSC under nitrogen purge at 40 ml/min.

Experimental observations suggest no substantial difference in solubility due to variation of the diamine portions (BAPP and APB). However, APB based polyimides exhibited lower inherent viscosities in NMP compared with those of BAPP-based ones as shown in Table 2. This suggests a difference in the reactivity of the diamines such that BAPP is more reactive than APB. It is also possible that the noted difference in the inherent viscosity may result from changes in the equilibrium chain conformations in different solutions. Further experiments are necessary to distinguish these two possibilities.

3.2. Glass transition and relaxation processes

The glass transition temperatures measured via DSC are also given in Table 2. BAPP-based polyimides exhibit a T_g which is approximately 50°C higher than that of APB-based polyimides. We speculate that the molecular weight difference of the polyimides alone may not cause such large difference in T_g (over 50°C). This suggests that the isopropylene segment in BAPP results in a greater restriction of segmental motion in the polyimide backbones than the ether linkages in APB. The restriction of molecular motion in polyimide backbones may also result from the differences of dianhydride structures. It is evident

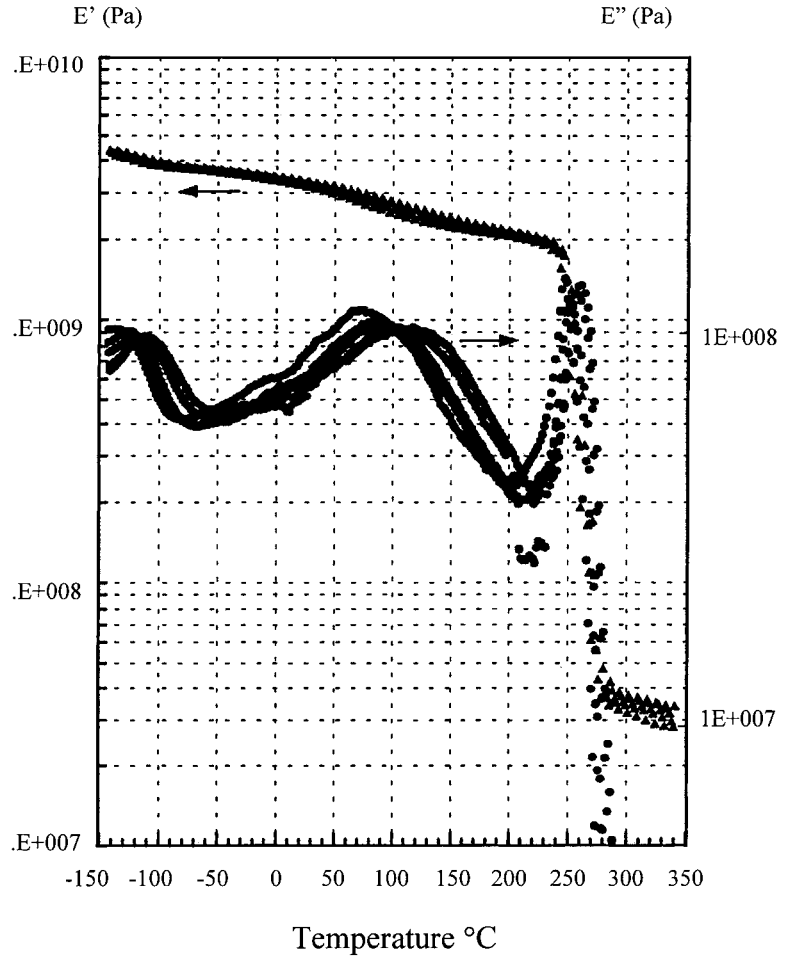

Fig. 1. E' and E'' changes with temperature for 6FDA–BAPP at different frequencies from 0.1 and 10 Hz.

that the T_g is in the sequence of 6FDA > BPDA > BTDA > ODPA-based polyimides for both diamines. It should be noted that the onset of cooperative motion associated with T_g in two 6FDA-based polyimides may further be delayed due to strong polar forces arising from the CF_3 groups.

The relaxation processes of these aromatic polyimides have been investigated with DM experiments. As an example, Figs. 1 and 2 show the relaxation spectrum of 6FDA-BAPP in terms of E′ and E″ changes and tan δ changes with temperature at two frequencies (0.1 and 10 Hz). Three relaxation processes are observed for all of the polyimides studied. A γ relaxation process appears between $-80^{\circ}C$ and $-120^{\circ}C$, followed by a β relaxation at 80–120°C. At the higher temperature (240–280°C), an α relaxation process is found. The α relaxation corresponds to the glass transition temperature observed from DSC measurements, although the α relaxation determined from DM exceeds the T_g from DSC by 10–15°C due to the frequency effect. Thus, both the β and γ processes are defined as subglass transition relaxation. A more careful study indicates that the intensities of the tan δ (associated with relaxation strength) differ for polyimides with varying chemical structures in three relaxation processes. This suggests that the relaxation strengths of the polyimides are also structure dependent. Fig. 3 offers a comparison of two tan δ curves for

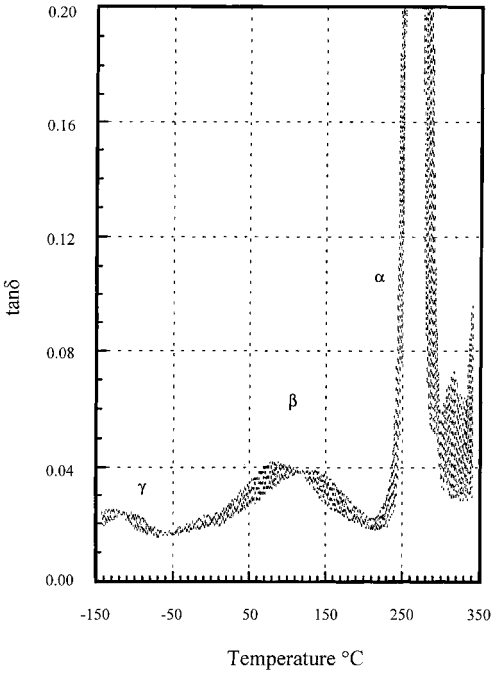

Fig. 2. Two tan δ curves for 6FDA–BAPP at different frequencies from 0.1 to 10 Hz.

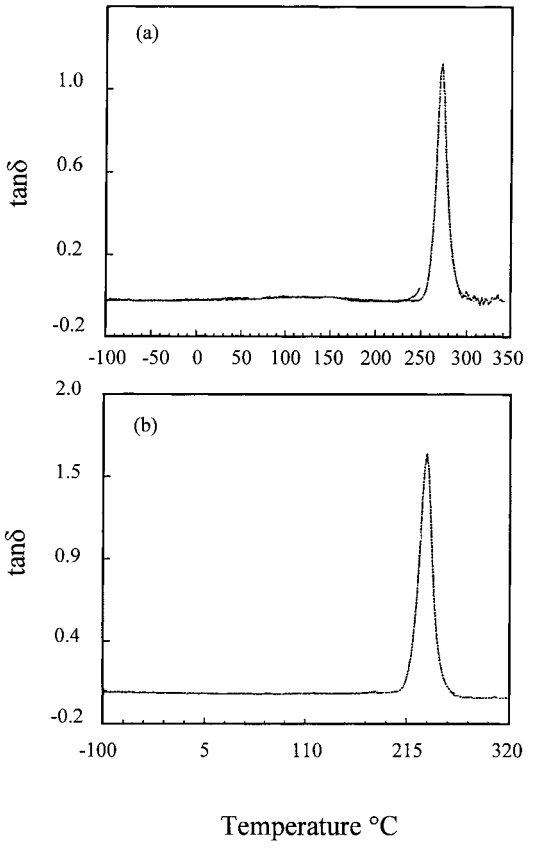

Fig. 3. Two tan δ curves with temperature for 6FDA–BAPP (a) and 6FDA–APB (b) at a frequency of 1 Hz.

6FDA–BAPP and –APB at 1 Hz. It is clear that APB based polyimides exhibit higher relaxation strengths than the BAPP-based polyimides at the α relaxation, which is associated with either a higher E'', a lower E' or both.

By assuming an Arrhenius relationship, one may calculate the activation energy for each polyimide from the frequency dependence of E'' peak temperatures for the three relaxation processes. The results are listed in Table 3. It is important to note that the WLF analysis rather than the Arrhenius approach must be used to describe the α relaxation behavior, suggesting that the α relaxation is not a spectrum with a single relaxation frequency. Within a narrow frequency range (i.e. three to four orders of magnitude) however, the Arrhenius approach can be applied to the α relaxation as a first approximation to obtain an apparent activation energy. On the other hand, for the motion associated with a subglass transition relaxation, the Arrhenius approach is well suited to describe the relaxation process. It is evident that the activation energies of the γ relaxation are similar for both series of polyimides, ranging from 35 to 50 kJ/mol. The activation energies for the β relaxation range between 120 and 140 kJ/mol. For the α relaxation, the apparent activation energies of APB-based polyimides are 770–870 kJ/mol, which are lower than those in BAPP-based polyimides (around 990 kJ/mol). This may be indicative of the effect of an ether linkage in APB on the molecular motion of polyimide backbone. Generally speaking, it is found that the T_g for BAPP-based polyimides exceeds that of APB-based polyimides by 40°C in the presence of the same dianhydride (Table 3). The difference in T_g of BTDA–BAPP measured by DSC and DM as shown in Tables 2 and 3 is expected since the glass transition temperature is also frequency-dependent. Only in the limit of very low frequency, can the T_g measured by DM be comparable to that observed with DSC.

Table 3
Dynamic mechanical properties of polyimides[a]

Polyimides	α		β		γ	
	E_a (kJ/mol)	T_p (°C)	E_a (kJ/mol)	T_p (°C)	E_a (kJ/mol)	T_p (°C)
ODPA–APB	770	191	138	115	41	−83
BTDA–APB	777	215	133	95	46	−90
BPDA–APB	864	219	140	122	45	−95
6FDA–APB	848	226	124	118	38	−106
ODPA–BAPP	989	244	134	94	42	−110
BTDA–BAPP	984	248	130	79	44	−106
BPDA–BAPP	985	262	132	94	43	−107
6FDA–BAPP	989	266	123	103	38	−115

[a] Activation energies were determined by using the Arrhenius relationship. Transition temperatures were determined as the peak of tan δ as function of temperature at 1 Hz.

For the γ and β relaxation processes, the Stark-weather approach was used to determine the cooperativity of the molecular motion [17,18]. If the molecular motion is non-cooperative in nature, the activation energies of the β and γ relaxation processes may be separated into activation enthalpy (ΔH^+) and activation entropy (ΔS^+) by using the Eyring theory of absolute reaction rates. The Arrhenius activation energy, E_a, can be written as

$$E_a = RT[1 + \ln(k/2\pi h) + \ln(T/f)] + T\Delta S^+, \quad (1)$$

where R is the gas constant, k and h, the Boltzmann and Planck constants, and f, the frequency. Stark-weather has reported that for many relaxation processes, particularly those involving submolecular fragments moving independently of one another, the activation entropy is close to zero [17,18]. Assuming that the activation entropy is zero, the frequency is 1 Hz, and the relaxation occurs at a temperature T' (K) at this frequency, the E_a then follows a simple, almost linear dependence on temperature:

$$E_a = RT'[1 + \ln(k/2\pi h) + \ln T']. \quad (2)$$

The extent to which the activation energy exceeds this value is equal to $T\Delta S^+$. Thus, Eq. (2) defines an effective low limit for the activation energy of viscoelastic relaxation [17]. Fig. 4 shows the relationships between the activation energy and temperature. The linear line represents the data calculated following Eq. (2), and the points are the experimental data. Comparison of the data with the line permits evaluation of the cooperativity of the molecular motion. It is evident that the γ relaxation processes involve non-cooperative motion. However, the β relaxations possess higher activation energies compared with those of the low limit of the activation energy (linear line in Fig. 4), indicating that these β relaxation processes involve the cooperative motion.

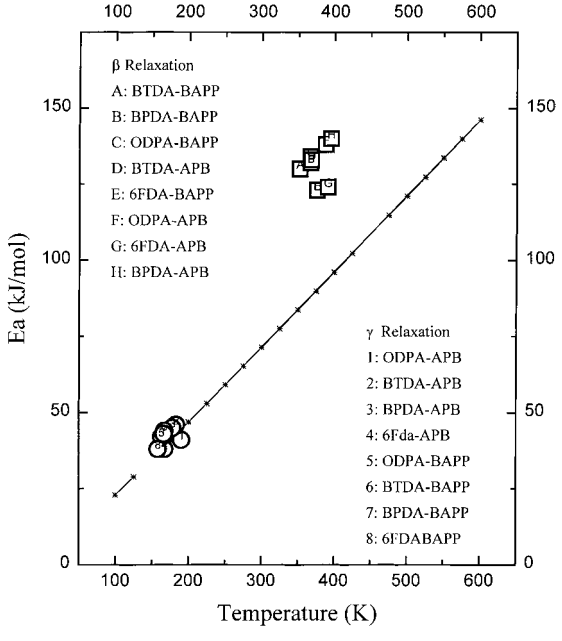

Fig. 4. Relationships of the effective lower limit for the activation energies calculated following Eq. (2) in the text and temperatures. The experimental data observed for the polyimides is also included.

Table 4
Mechanical properties and fracture toughness of neat polyimides[a]

Polyimides	E (GPa)	σ_y (MPa)[b]	K_{IC} (Mpam$^{1/2}$)	G_{IC} (J/m^2)
ODPA–APB	3.79	132.7	2.66	1638
BTDA–APB	3.93	138.1	3.15	2216
BPDA–APB	3.65	128.5	4.18	2201
6FDA–APB	3.14	100.6	2.57	1846
ODPA–BAPP	3.08	94.4	2.79	2218
BTDA–BAPP	3.18	98.2	2.80	2110
BPDA–BAPP	3.00	99.5	2.73	2180
6FDA–BAPP	2.90	88.2	2.82	2406

[a] Fracture toughness was measured by using double torsion (DT) method at room temperature with the crosshead speed of 0.5 mm/min.
[b] σ_y – tensile yielding stress were performed on the Tensometer/T-10, Monsanto, with the cross-head speed of 5 mm/min at room temperature.

At present, the molecular origin of these subglass relaxation processes is not exactly known. However, it is believed that they are associated with a non-cooperative or less cooperative motion of certain groups in the chain structures. For example, in the fully aromatic polyimides, it has been suggested that the β relaxation is coupled with a molecular motion in diamine portions of the backbones [19]. Some reports proposed that the origin of the γ relaxation is due to the moisture absorption [20–22]. However, others indicated that this relaxation is associated with a low temperature phenylene ring π-flippy motion [23]. Further experimental study in C-13 solid state nuclear magnetic resonance will be necessary to identify the origin of the molecular motion associated with these relaxation processes.

3.3. Mechanical properties of the polyimides and copolyimides

Table 4 presents the mechanical properties of the polyimides tested including tensile modulus (E), yielding stress (σ_y) and fracture toughness (K_{IC} and G_{IC}). As shown in Table 4, the moduli of APB-based polyimides are generally higher than those of BAPP-polyimides. This indicates that the moduli of polyimides in these systems are more affected by the diamine portions than the dianhydrides. Interestingly, the yielding stress of the polyimides shows the same trend as the modulus data. However, the toughness data does not demonstrate a notable tendency with variation of either the dianhydrides or diamines. Quantitative correlation of the mechanical properties with the chemical structures of polyimides is usually difficult to obtain, although these polyimides are amorphous polymers and do not exhibit multiple levels of the phase morphology such as crystal phase which may further complicate correlation of structures to the properties. Thus, the mechanism for the lower moduli and yielding stresses in BAPP-based polyimides remains beyond the scope of this study.

Table 5
Properties of copolyimides based on ODPA–APB–BAPP

Molar Ratio (ODPA–APB–BAPP)	T_g (°C)	E (GPa)	σ_y (MPa)
10–10–0	181	3.79	132.7
10–5–5	196	3.35	120.2
10–3–7	211	3.18	106.2
10–0–10	232	3.08	94.4

In order to elucidate the influence of the diamine on the modulus and yielding stress of polyimide, copolyimides were also synthesized. As shown in Tables 5 and 6, it is clear that the modulus and yielding stress decrease as the composition of BAPP in the copoly-

Table 6
Properties of copolyimides based on BPDA–APB–BAPP

Molar Ratio (BPDA–APB–BAPP)	T_g (°C)	E (GPa)	σ_y (Mpa)
10–10–0	202	3.65	128.5
10–5–5	224	3.40	118.0
10–3–7	237	2.94	106.2
10–0–10	250	2.93	99.5

imides increases. However, the glass transition temperature of these copolyimides exhibits an opposite trend. These observations are consistent with the thermal and mechanical properties observed in the homopolymers. Therefore, it is possible to tailor the chemical structure to obtain desired macroscopic properties of thermoplastic polyimides, which are important for improving toughness of epoxy resin. One should note that lower yielding stress of a polyimide in an epoxy matrix might induce either plastic yielding or void formation within a second phase during fracture. The energy dissipation will then be increased through this toughening mechanism. At ambient temperature, the improvement of toughness is mainly attributed to the existence of the sub-glass transitions which absorb impact energies. It should also be noted that the sub-glass and glass transition temperatures decrease when increasing external stress is applied to these polyimides.

4. Conclusion

Dianhydride and diamine modifications can enhance the solubility of polyimides. However, only the polyimides synthesized from 6FDA or ODPA with the diamines can be dissolved in Epon 828 monomers. Aromatic polyimides exhibit three relaxation processes (γ, β, and α processes). Both of the γ and β processes are subglass relaxations. The γ process involves non-cooperative motion, while the β process is associated with a cooperative motion. The α relation process is the glass transition process. For the mechanical properties, the isopropylene segment in the polyimide backbone is most likely responsible for the decrease of modulus and yielding stress as well as the increase in T_g of the polyimides. The copolymer study clearly indicates that a qualitative additivity of the thermal and mechanical properties in the systems studied and could be used to molecularly design the proper chemical structures to obtain the desired toughening agents for epoxy resins.

Acknowledgements

This work was supported by NSF Center for Molecular and Microstructure of Composites.

References

[1] J.L. Hedrick, I. Yilgor, G.L. Wilkes, J.E. McGrath, Polym. Bull. 13 (1985) 201.
[2] S.G. Chu, B.J. Swetlin, H. Jabloner, US Patent 4 656 208 (1987).
[3] Z. Fu, Y. Sun, Polym. Prepr. (Am. Chem. Soc. Div. Polym. Chem.) 29(2) (1988) 177.
[4] C.B. Bucknall, I.K. Partridge, Polymer 24 (1983) 639.
[5] R.S. Raghava, J. Polym. Sci., Polym. Phys. Ed. 26 (1988) 65.
[6] C.B. Bucknall, A.H. Gilbert, Polymer 30 (1989) 213.
[7] J.A. Cecere, J.E. McGrath, Polym. Prep. (Am. Chem. Soc. Div. Polym. Chem.) 27(1) (1986) 299.
[8] G.S. Bennett, R.J. Farris, S.A. Thompson, Polymer 32 (1991) 1633.
[9] J.K. Kim, R.E. Robertson, Polym. Mater. Sci. Eng. 27 (1992) 161.
[10] S.Z.D. Cheng, S.K. Lee, J.S. Barley, S.L.-C. Hsu, F.W. Harris, Macromolecules 24 (1991) 1803.
[11] S.K. Lee, S.Z.D. Cheng, S.L.-C. Hsu, C.J. Lee, F.W. Harris, T. Kyu, J.C. Yang, Polym. Interl. 30 (1993) 115.
[12] P.J. Flory, J. Chem. Phys. 10 (1942) 51.
[13] M.L. Huggins, J Am. Chem. Soc. 64 (1942) 1712.
[14] T.L. St. Clair, in: D. Wilson, F.D. Stenzenberger, P.M. Hergenrother (Eds.), Polyimides, Blackie, Chapman & Hall, New York, 1991, pp. 58–78.
[15] E.P. Savitski, F.-M. Li, S.-H. Lin, K.W. McCreight, F.W. Harris, S.Z.D. Cheng, S.C. Man Kwan, C. Wu, Internat. J. Polym. Anal. Charact. 4 (1997) 153.
[16] S.C. Man Kwan, C. Wu, F. Li, E.P. Savitski, F.W. Harris, S.Z.D. Cheng, Macromol. Chem. Phys. 198 (1997) 3605.
[17] H.W. Starkweather Jr., Polymer 32 (1991) 2443.
[18] H.W. Starkweather Jr., P. Avakian, Macromolecules 22 (1989) 4060.
[19] F.E. Arnold Jr., K. Bruno, D.-X. Shen, M. Eashoo, C.J. Lee, F.W. Harris, S.Z.D. Cheng, Polym. Eng. and Sci. 33 (1993) 1373.
[20] R.M. Ikeda, J. Polym. Sci. Polym. Lett. Ed. 4 (1966) 353.
[21] G.A. Bernier, D.E. Kline, J. Appl. Polym. Sci. 12 (1968) 593.
[22] J.K. Gillham, K.D. Hallock, S.J. Stanknicki, J. Appl. Polym. Sci. 16 (1972) 2595.
[23] S.Z.D. Cheng, T.M. Chalmers, Y. Gu, F.W. Harris, J.-L. Cheng, J. Konieg, Macromol. Chem. Phys. 196 (1995) 1439.